Geophys. J. Int. (2006) **167,** 1447–1460 doi: 10.1111/j.1365-246X.2006.03158.x

Large igneous provinces generated from the margins of the large low-velocity provinces in the deep mantle

Trond H. Torsvik,[1]* Mark A. Smethurst,[1] Kevin Burke[2] and Bernhard Steinberger[1]

[1]*Center for Geodynamics, Geological Survey of Norway, Leiv Eirikssons vei* 39, N-7491 *Trondheim (Norway)*
[2]*Department of Geosciences, University of Houston,* 312 S&R1 *Houston* Tx 77204-5007, *GL and DTM, Carnegie Institution of Washington,* 5241 *Broad Branch Road, Washington* DC 20015, *USA, and School of Geosciences, University of the Witwatersrand,* WITS, 2050*, South Africa*

Accepted 2006 July 27. Received 2006 July 24; in original form 2006 February 27

SUMMARY

There is a clear correlation between downward projected large igneous province (LIP) eruption sites of the past 200 Myr and the margins of the large low-velocity provinces (LLVPs) at the base of the mantle. We established this correlation by using palaeomagnetic as well as fixed and moving hotspot reference frames. Our finding indicates that the majority of the LIPs have been generated by plumes that rose from the D″ zone at the edges of the LLVPs. Most LIP eruption sites project radially downwards to the core–mantle boundary (CMB) within $\pm 10^{\circ}$ of the 1 per cent slow shear wave velocity contour in the SMEAN tomographic model. Steep shear wave velocity gradients have been mapped near the CMB along much of the lengths of the LLVP margins close to that contour which marks a faster/slower boundary (FSB) within the D″ zone. The observation that eruption sites of LIPs as old as 200 Myr can be linked to this prominent present day seismic structure shows that the FSBs of the two LLVPs have occupied their current positions for at least as long and that the process that leads to the generation of deep-seated plumes has been localized on the FSBs at the margins of the African and Pacific LLVPs for the same interval. The persistence of the LLVPs over 200 Myr is consistent with independent evidence that they are compositionally distinct and are not just simply hotter than the material making up the rest of the D″ zone.

Key words: core–mantle boundary, hotspots, large igneous provinces, large low-velocity provinces, palaeomagnetism, reconstructions, seismic tomography.

1 INTRODUCTION

Higher-velocity regions in tomographic models of the Earth's mantle, for example in those of Becker & Boschi (2002), occupy regions which geodynamic interpretations, such as that of Richards & Engebretson (1992), have suggested contain graveyards of ancient subducted material. In contrast low-velocity regions of the deep mantle, the large low-velocity provinces (LLVPs) of Lay (2005), have been suggested to contain the sources of mantle plumes but deep plume models are controversial and alternative models associate all hotspot volcanism with shallow tectonic processes (Foulger *et al.* 2005). We have recently demonstrated that large igneous provinces (LIPs, Fig. 1) of the past 200 Myr, when restored by palaeomagnetic rotation to their positions with respect to the spin-axis at the time of their eruption, become concentrated radially above the regions close to the CMB that are occupied in tomographic models by the slower parts of the D″ zone (Burke & Torsvik 2004). It is perhaps not yet time to abandon the idea of deep mantle plumes!

2 LOCATION AND SIGNIFICANCE OF LIP ERUPTION SITES

LIPs extend over huge areas (Fig. 1; Table 1) that commonly mark not the site of a plume from deep within the mantle but the location of material that has propagated horizontally, within the lithosphere from a plume (Sleep 1997). Magma from plume eruptions has been shown to have propagated horizontally for more than 1000 km from eruption sites (e.g. Marzoli *et al.* 1999). We have reviewed the LIP locations of Eldholm & Coffin (2000; see also Burke & Torsvik 2004) with long distance magma propagation in mind and have found it necessary to make only small changes in mapped plume eruption locations. We have, however, made some significant changes to the ages (Table 1). New marine magnetic data (Jokat *et al.* 2003) demonstrate that Maud Rise was erupted close to 125 Ma and not at 73 Ma. The 90 Ma age for Ontong Java 2 has been shown to be misleading because there was no renewed eruption at that time (Parkinson *et al.*

*Also at: Institute for Petroleum Technology and Applied Geophysics, Norwegian University of Science & Technology, N-7491 NTNU (Norway), and School of Geosciences, University of the Witwatersrand, WITS, 2050, South Africa. E-mail: trond.torsvik@ngu.no

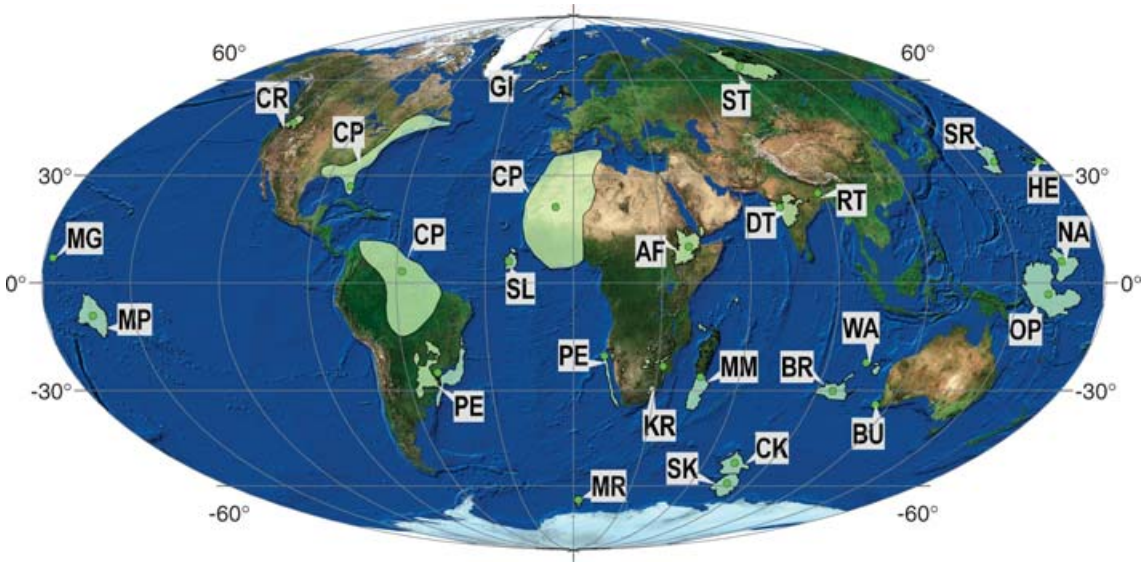

Figure 1. Large igneous provinces (LIPs) and their eruption centres. The positions of some of the centres are speculative. LIP names are listed in Table 1. Outlines of the CAMP plume (CP) are generalized and liberal in their inclusion of igneous bodies. Mollweide projection.

2002; Chambers *et al.* 2004; Bergen 2004). This change requires that Ontong Java, previously subdivided into two LIPs, has to be considered as a single LIP erupted at around 121 Ma. We excluded two LIPs (Argo Margin & Gascoyne) of the Australian margin from Table 1 because their ages are not well constrained.

The locations of plume eruption sites at the Earth's surface (Fig. 1; Table 1) may not be the places where the plume heads impinged on the base of the lithosphere so that locating plume eruption sites with higher resolution than *ca.* 500 km may be unrealistic. We found that six of the LIPs that our earlier work indicated were of deep origin (CAMP, Karroo, Tristan, Rajmahal, South Kerguelen, Deccan and Iceland; see Burke *et al.* 2003; Burke & Torsvik 2004) erupted into existing rifts. Sleep (1997) provided a plausible explanation for that observation. He considered (1) that a plume head might impinge anywhere on the base of the lithosphere, (2) that magma generated at the site of such an impingement could travel buoyantly along the base of the lithosphere by what he called 'upside-down drainage' to a place, such as an existing rift, where the lithosphere was already thin and (3) that a LIP derived from the plume which had impinged far away could then erupt. Fortunately more than 700 rifts have been mapped within the continental lithosphere (Sengor & Natalin 2001) so that upside down drainage is unlikely to have to travel for more than *ca.* 500 km before initiating LIP eruption.

3 GLOBAL TOMOGRAPHIC MODELS AND THE CMB

Our interest has been in observing how and whether the downward projected locations of LIPs and hotspots can be related to the deep mantle structure discerned tomographically. Our findings are somewhat sensitive to which tomographic models we choose and we have concentrated on shear wave models because structure within the D″ zone is better seen in those models. Estimates of the vertical and horizontal extent of heterogeneities, shear wave velocities and gradients in shear wave velocities are not entirely independent in the models and, as with all tomography, spatial resolution is highly variable. With these limitations in mind we have examined and compared most global shear wave tomographic models at the CMB (2900 km depth). Our preferred SMEAN model (fig. 2, Becker & Boschi 2002) is based on the NGRAND, S20RTS and SB4L18 models (Fig. 3).

Two LLVPs (low δV_s regions, the LLVPs of Lay 2005) are the most prominent features of all global shear wave tomographic models (Figs 2 and 3). At their bases the two LLVPs between them extend over about 25 per cent of the CMB. As the resolution of seismic tomography increases, internal coherency of the LLVPs may diminish, but the large-scale pattern will persist (Lay 2005). The relatively well-defined African and Pacific LLVPs, are isolated within the faster parts of the D″ zone. Richards & Engebretson (1992), Van der Voo *et al.* (1999) and many others have suggested that the faster regions are cooler because they contain subducted slab material while the two slower regions have escaped that refrigerating influence.

In Fig. 2 red-to-blue contours indicate the locations of approximately 50 features with horizontal shear wave velocity gradients above 0.16 per cent/degree (calculated from the SMEAN model of Becker & Boschi 2002). These very steep velocity gradients, all of which extend over $<10^\circ$, account for about a quarter of the full 5 per cent range of shear wave velocity variation at the CMB. The very steep velocity gradients are concentrated at the margins of the two LLVPs close to the 1 per cent slow contour. Less steep gradients, although still steeper than average, extend along much of the rest of the 1 per cent slow contours. The 1 per cent slow contours form faster/slower boundaries (FSBs) within D″ velocity structure. The concentration of steep gradients is better defined at the margin of the African LLVP than it is at the margin of the Pacific LLVP.

4 LIP LOCATIONS AT ERUPTION TIMES—METHODS

Burke & Torsvik (2004) restored 25 LIPs of the past 250 Myr to their initial eruption sites using the palaeomagnetic method. By assuming no relative motions between the Pacific and East Antarctica prior to 90 Ma and following plate-circuit procedures outlined by Norton

Table 1. Large igneous provinces (sorted by age) updated from Burke & Torsvik (2004). LIPs are restored to their emplacement positions according to four different reference frames as described in the text. Lat/Long is latitude/longitude. δV_S is extracted from the SMEAN shear wave velocity anomaly model at each of the emplacement positions. 1 per cent is distance in degrees from 1 per cent slow contour (minus if inside). Symbols are as used in figures. Note that the distance for the Siberian Traps is measured from a small local 1 per cent slow area. LIPs in bold are from the Pacific. δV_S and distance from the 1 per cent slow contour are calculated by *upward* projection of CMB tomography to the Earth's surface *without* considering plume advection; this introduces an error of unknown magnitude and in addition the locations of plume eruption sites at the Earth's surface may not be the places where the plume heads impinged on the base of the lithosphere so that locating plume eruption sites with higher resolution than ~500 km is unrealistic.

					Reference frame														
Large igneous province					Global Palaeomag.				Africa Fixed Hotspot				Africa Moving Hotspot				'Global moving' hotspot			
Name	Age	Symbol	Lat	Long	Lat	Long	δV_S	1 per cent	Lat	Long	δV_S	1 per cent	Lat	Long	δV_S	1 per cent	Lat	Long	δV_S	1 per cent
Columbia RB	15	CR	46.0	−119.0	45.6	249.1	1.1	48	47.3	243.6	0.9	50	46.7	245.2	0.9	49	48.5	244.0	0.9	51
Afar FB	31	AF	10.0	39.5	3.2	39.0	−0.1	5	4.6	34.8	−0.9	2	5.6	35.0	−0.7	3	4.5	36.4	−0.6	3
Greenland/Iceland	54	GI	69.0	−27.0	53.7	355.8	−0.3	11	59.2	353.3	−0.3	15	59.2	349.6	−0.4	15	63.0	353.3	−0.4	19
Deccan T	65	DT	21.0	73.0	−22.0	64.4	0.0	6	−20.5	56.2	−1.1	0	−18.7	58.4	−0.5	2	−17.4	55.2	−0.8	2
S. Leone R	73	SL	6.0	−22.0	−0.5	338.8	−0.6	6	1.8	332.3	−0.2	9	2.7	334.2	−0.5	7	4.7	331.8	−0.3	8
Madagascar/M	84	MM	−26.0	46.0	−45.6	44.6	−1.0	0	−46.3	36.9	−0.5	4	−40.5	39.5	−1.2	0	−41.7	35.9	−0.9	0
Broken R	95	BR	−30.0	96.0	−49.1	74.5	−1.7	−5	−49.9	69.0	−1.8	−9	−45.7	68.0	−2.1	−10	−46.3	65.3	−2.1	−12
Wallaby P	96	WA	−22.0	104.0	−44.5	88.9	−0.4	6	−44.5	83.0	−0.7	2	−41.8	82.0	−0.9	2	−41.8	79.2	−1.0	0
Hess R	99	HE	34.0	177.0	2.6	225.4	−0.7	1	6.4	216.4	−1.7	−5	1.1	220.3	−1.6	−4	3.2	218.4	−1.8	−6
C. Kerguelen	100	CK	−52.0	74.0	−48.1	69.4	−2.0	−9	−48.8	64.3	−1.9	−10	−45.4	63.3	−1.9	−13	−45.1	61.2	−1.8	−15
Nauru B	111	NA	6.0	166.0	−26.4	222.0	−1.8	−7	−26.9	202.6	−1.5	−8	−29.9	206.8	−1.5	−14	−24.1	211.6	−1.9	−18
S. Kerguelen	114	SK	−59.0	79.0	−55.6	58.5	−1.0	0	−48.0	63.2	−1.9	−12	−48.9	59.7	−1.7	−10	−44.1	60.3	−1.7	−16
Rajhmahal T	118	RT	25.0	88.0	−46.0	64.4	−1.9	−13	−36.4	63.8	−1.7	−5	−39.1	61.4	−1.8	−16	−32.7	61.8	−1.3	−2
Ontong JP	121	OP	−3.0	161.0	−38.2	219.7	−0.9	3	−39.0	190.5	−0.8	3	−40.4	197.1	−0.9	2	−32.0	209.4	−1.6	−13
Manihiki P	123	MP	−9.0	−164.0	−34.5	264.5	−0.5	7	−50.3	239.6	−0.4	28	−45.8	246.3	0.1	22	−37.6	253.2	0.0	12
Maud R	125	MR	−65.0	3.0	−50.3	0.5	−0.7	1	−55.9	10.2	0.3	6	−54.2	0.2	0.3	5	−51.3	11.8	−0.5	2
Parana-Etendeka	132	PE	−20.0	11.0	−29.5	352.4	−1.5	−9	−37.2	350.7	−1.4	−4	−33.6	344.4	−1.0	−1	−33.5	352.5	−1.4	−7
Bunbury B	132	BU	−34.0	115.0	−61.3	78.5	0.0	7	−46.7	78.7	−1.4	−2	−54.2	73.2	−1.3	−3	−44.5	75.5	−1.6	−4
Magellan R	145	MG	7.0	−177.0	−26.9	244.3	−1.1	0									−22.4	246.6	−1.2	−5
Shatsky R	147	SR	34.0	160.0	−4.0	219.0	−1.9	−7									5.6	227.0	−0.4	3
Karroo B	182	KR	−23.0	32.0	−38.9	20.7	−2.4	−7												
CAMP	200	CP	27.0	−81.0	3.4	346.4	−1.2	−2												
Siberian T	251	ST	65.0	97.0	58.1	58.2	−0.2	6												

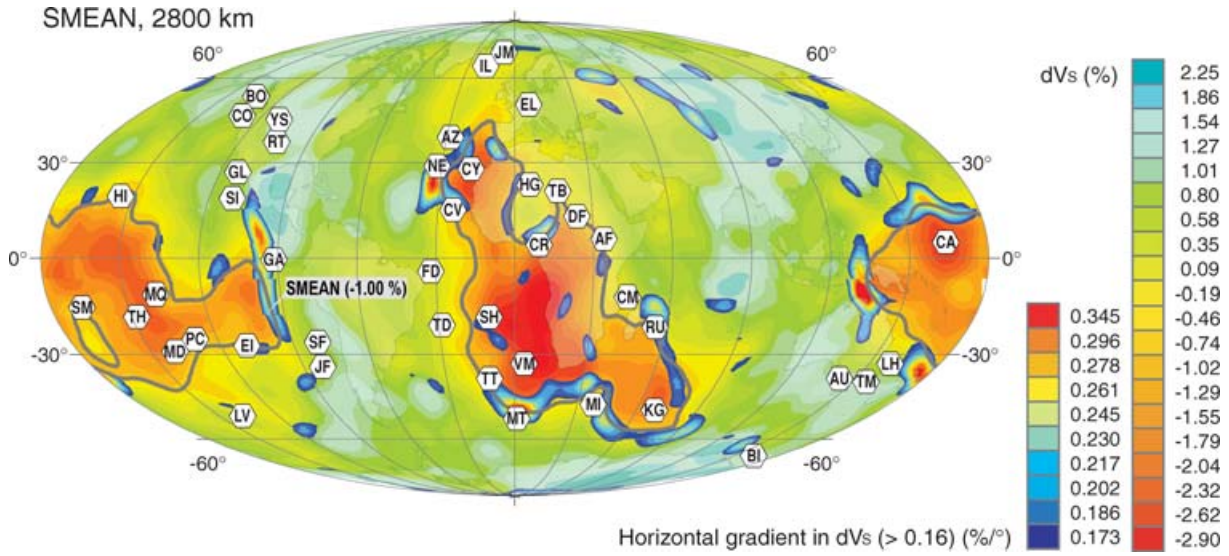

Figure 2. Hotspots (Steinberger 2000) plotted on the SMEAN shear wave velocity anomaly model for 2800 km depth of Becker & Boschi (2002). Hotspot names are listed in Table 2. Velocity anomalies (δV_s) are expressed in percent. Blue denotes regions with high velocity and red with low velocity. The −1 per cent contour (1 per cent slow) is shown in grey. Horizontal gradients in shear wave velocity anomaly (per cent δV_s/degree) are indicated where they exceed 0.16 per cent/degree.

(2000) they restored Pacific LIPs to African coordinates. We here describe their method and our three other ways of restoring the LIPs of Table 1 to their locations at the time they were erupted and compare the results of the four approaches. All four approaches have in common that we first establish an 'absolute' motion of Africa, and then apply relative plate motions described in Torsvik *et al.* (2006) to rotate LIPs into their original eruption positions with respect to a restored Africa. Throughout this paper we also use Steinberger *et al.* (2004) plate circuit Model 2 that connects Africa and the Pacific via East Antarctica–Australia–Lord Howe Rise for times between 46.3 and 83.5 Ma. Before 83.5 Ma, we either assume no further motion between Pacific, East and West Antarctic plates (first three cases) or treat the Pacific hemisphere separately (last case).

4.1 African fixed hotspot method

Based on volcanic hotspot tracks in the Indo-Atlantic realm, Müller *et al.* (1993) calculated best-fit plate rotations relative to present-day hotspots since the Cretaceous (*ca.* 130 Ma). For older times (>83.5 Ma) this model is subject to large uncertainties because it is based on only two hotspot tracks. We have tested this model and revised it according to more recent timescales (Torsvik *et al.* 2006) (Table 1, Fig. 4).

4.2 African moving hotspot method

Hotspots may not be fixed relative to each other (e.g. Steinberger *et al.* 2004) and the hotspot frame can in that case be replaced by a mantle reference frame in which the motion of hotspots in a convecting mantle is considered. Here, the 'absolute' position of Africa back to 130 Myr is determined by its motion with respect to African hotspots, as in (4.1) above, but the position of each hotspot is adjusted for the effects of mantle convection. For the purpose of this paper we used the 'smooth' model of O'Neill *et al.* (2005) (Table 1, Fig. 5).

4.3 Global palaeomagnetic method

The palaeomagnetic frame has the advantage that we can extend our analysis back to 251 Ma (i.e. Siberian Traps). Furthermore, it is totally independent of both the hotspot and mantle frames. To optimize the palaeomagnetic method, however, the choice of reference plate is critical. If there is reason to suppose that a particular continent has moved little longitudinally since the time represented by the reconstruction, that continent should be used as the longitudinally fixed reference plate (Burke & Torsvik 2004; Torsvik *et al.* 2006). Africa meets this criterion and is therefore used as the reference plate in order to minimize longitudinal uncertainties in palaeomagnetic reference frames and compare them directly with hotspot and mantle frames (Table 1, Fig. 6). This new global palaeomagnetic reference frame is detailed in Torsvik *et al.* (2006).

4.4 Global moving hotspot frame

Although similar to (4.2), this model is global: the Pacific and Indo-Atlantic domain hotspots have been combined to calculate the 'absolute' African and Pacific plate motion. This frame goes back to 83.5 Ma, but has been extended here based on *separate* Africa and Pacific *fixed hotspot* frames. The African plate motion calculated here differs from Steinberger *et al.* (2004) in that the same relative plate motions between Antarctica and South Africa and Australia and Antarctica as in the other parts of this paper are used, and they are slightly different from those that had been used by Steinberger *et al.* (2004) (detailed in Torsvik *et al.* 2006). For the African plate, we extend the reference frame prior to 83.5 Ma with the same rotation rates as in the revised African fixed hotspot reference frame of Section 4.1. (Table 1, Fig. 7).

For the Pacific plate, we extend the reference frame back in time with the same rotation rates as in the Pacific fixed hotspot frame of Duncan & Clague (1985). This combined approach shows that the restored Pacific LIPs (Fig. 7) compare reasonably well with the palaeomagnetically reconstructed LIPs (Fig. 6) showing that our

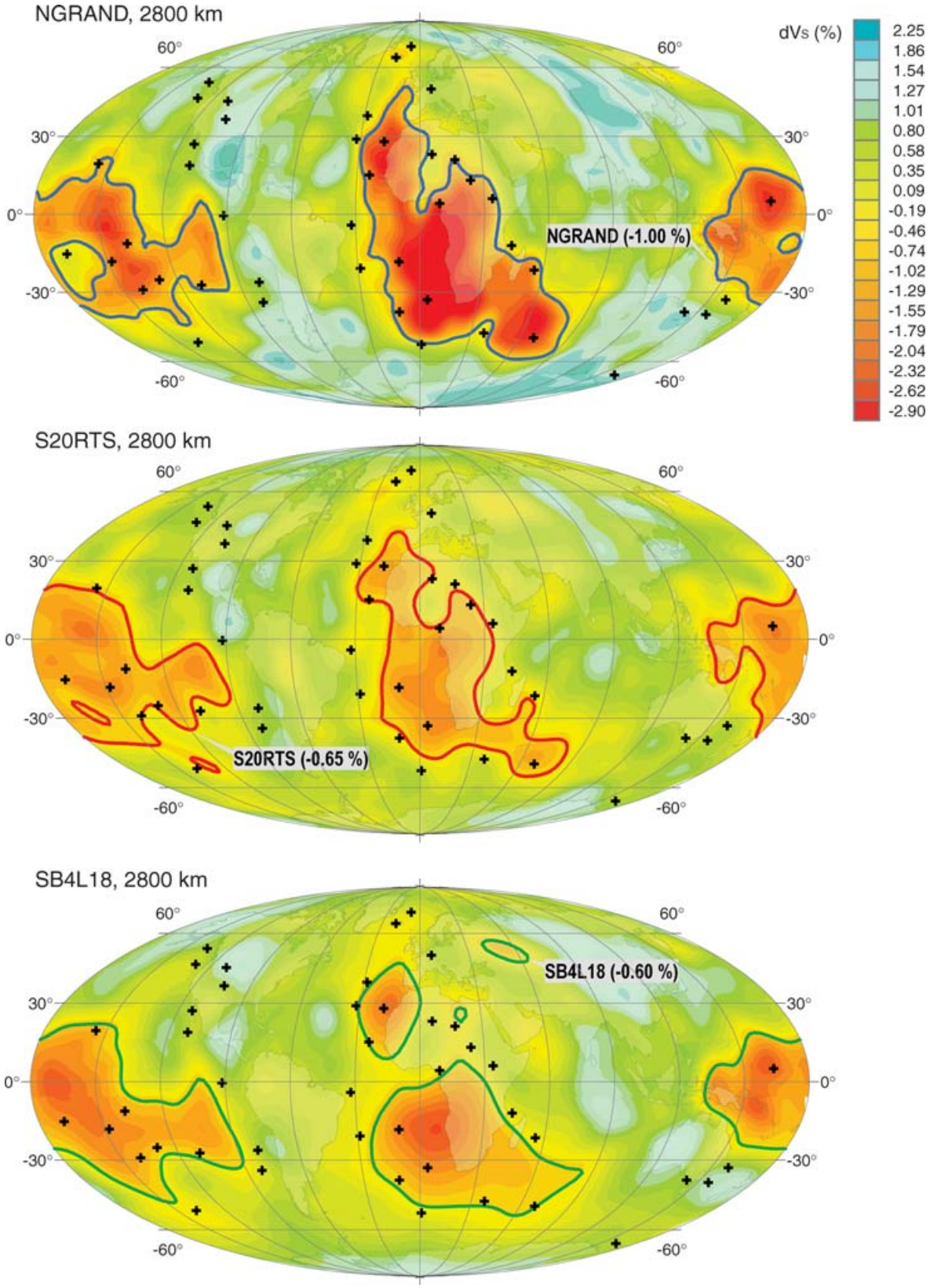

Figure 3. The NGRAND (Grand 2002), S20RTS (Ritsema *et al.* 1999) and SB4L18 (Masters *et al.* 2000) shear wave velocity models for 2800 km depth. The models were combined by Becker & Boschi (2002) to produce the SMEAN model of Fig. 2. All models are displayed using the same colour scale. NGRAND is contoured at −1 per cent, S20RTS at −0.65 per cent and SB4L18 at −0.6 per cent. All three contours are similar in form to the −1 per cent contour for SMEAN in Fig. 2. Hotspots are indicated by crosses.

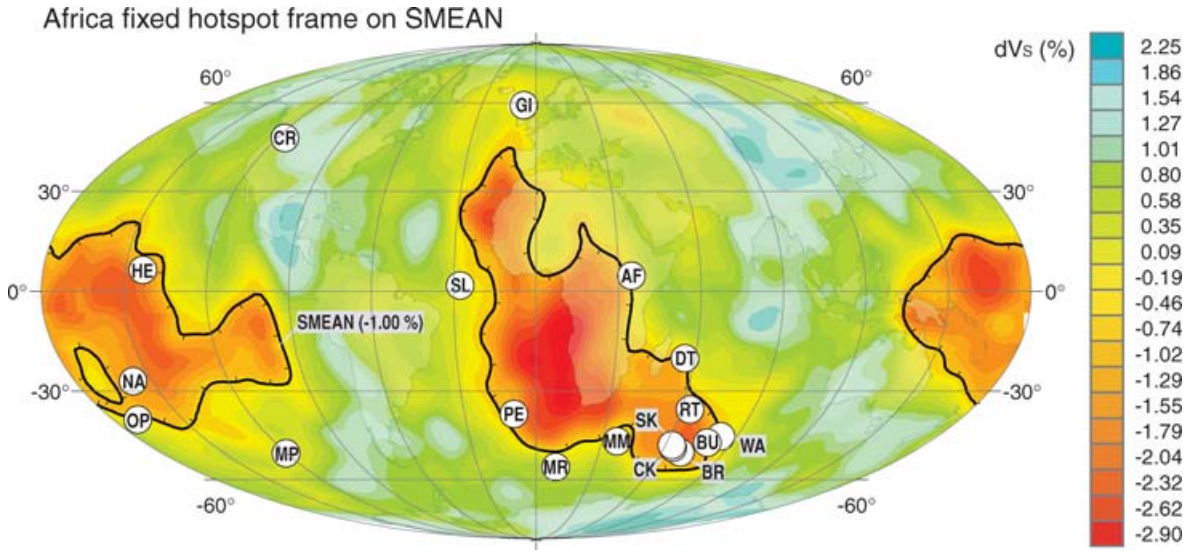

Figure 4. LIPs restored to their original eruption locations with respect to the fixed African hotspot reference frame of Müller *et al.* (1993) as updated by Torsvik *et al.* (2006) (Table 1). This reference frame is viable back to 130 Ma.

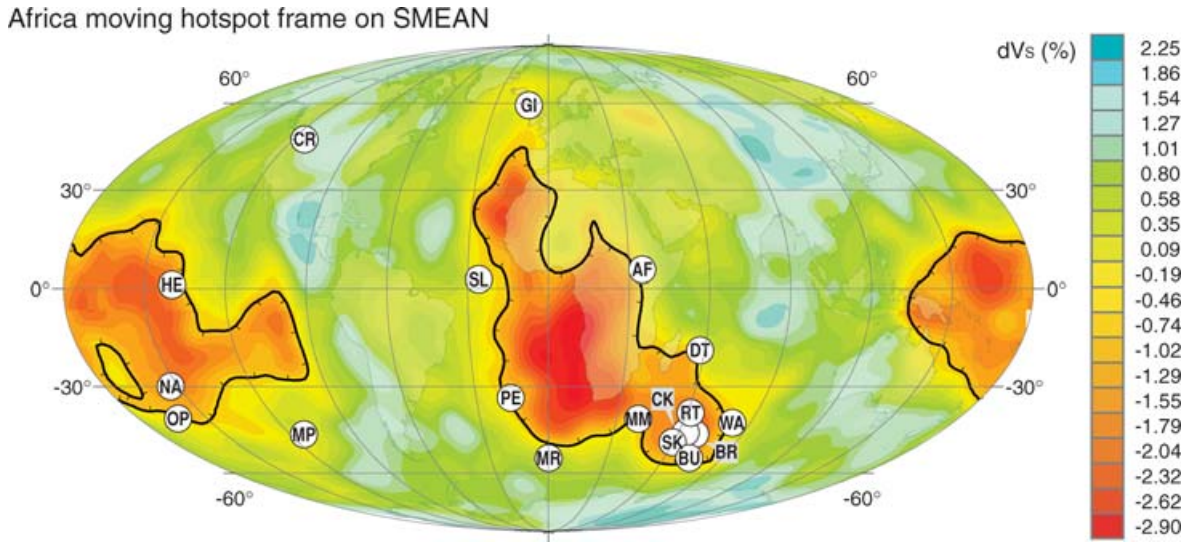

Figure 5. LIPs restored to their original eruption locations with respect to the smoothed Africa mantle reference frame of O'Neill *et al.* (2005) (Table 1). This restoration is viable back to 130 Ma (originally reported back to 120 Ma—here extrapolated to 130 Ma).

assumption of insignificant relative movements between Pacific and East Antarctica prior to 83.5 Ma is a *reasonable* approximation.

4.5 Palaeomagnetic versus mantle frames and direct palaeomagnetic observations

Due to errors in both palaeomagnetic and mantle reconstructions, restored LIP eruption sites for the last 100 Myr probably overlap within errors at the 95 per cent confidence level (Torsvik *et al.* 2006). Substantially larger differences are recognized for the Early Cretaceous (Table 1) and this is clearly reflected when we calculate the standard deviation for restored LIP latitudes only (Fig. 8a). In Fig. 8(b) we compare the restored *latitudes* of all LIPs determined by using all reference frames outlined above as well as direct palaeomagnetic observations when available. Except for the Ontong Java (*ca.* 121 Ma) LIP there is a reasonable correspondence between the global palaeomagnetic frame and observed latitudes. There is a clear discordance (14°) between latitudes derived from the palaeomagnetic frame and observed palaeomagnetic data from Ontong Java; the global (Pacific) mantle frame reduces this discordance to 8°. Fig. 8 also shows that all LIPs in the 200 to 65 Myr range were erupted at equatorial (4 LIPs) or intermediate southerly latitudes (15 LIPs). This hemispherical asymmetry could be: (1) a preservation artefact, (2) a surface distribution controlled by structure in the deep mantle or (3) a result of a combination of these causes.

5 LIP AND HOTSPOT LOCATIONS AT ERUPTION TIME—LINKS TO THE DEEP MANTLE

All restoration methods rotate most LIPs back to eruption sites near to locations radially above the FSBs of the African and Pacific LLVPs in the SMEAN model (Table 1, Figs 4–7). Davaille et al. (2005) using different rotation methods reported a similar result for

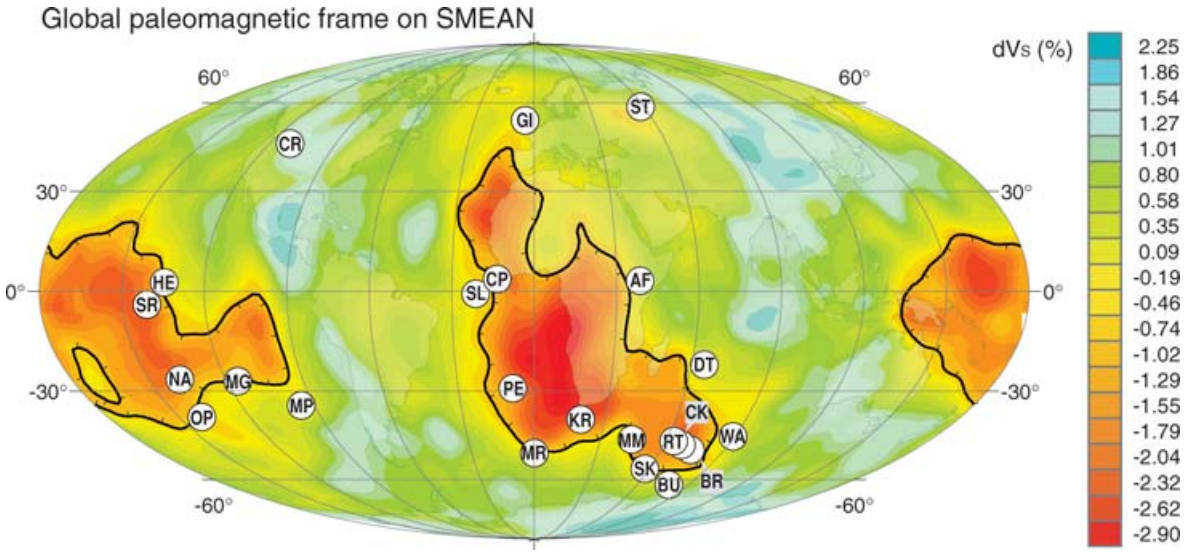

Figure 6. LIPs restored to their original eruption locations with respect to the global palaeomagnetic reference frame of Torsvik *et al.* (2006). This model is viable back to 320 Ma (initial formation of the Pangea Supercontinent).

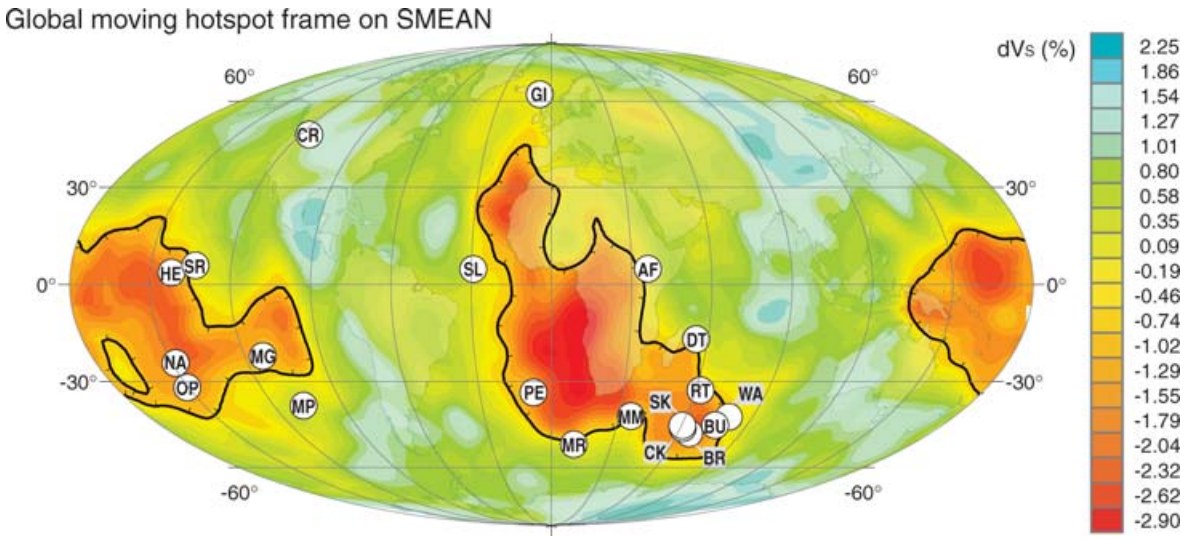

Figure 7. LIPs restored to their original eruption locations with respect to the global mantle frame of Steinberger *et al.* (2004) as later updated by Torsvik *et al.* (2006) (Table 1). This frame is truly global back to 83.5 Ma; during time intervals prior to that, Pacific Ocean LIPs are restored to their original eruption locations with rotation rates from a fixed hotspot frame back to 150 Ma (Duncan & Clague 1985), and other LIPS are restored with rotation rates from the African fixed hotspot reference frame back to 130 Ma (modified after Müller *et al.* 1993).

the African LLVP but did not consider the Pacific LLVP. No matter which method we used, the Columbia River LIP remained far from the FSBs. Excluding Columbia River, the mean angular deviation of the restored LIPs from the FSBs, that is from the 1 per cent slow contour, is 7° (Fig. 9; in the Pacific the average deviation is 8°). Four different restoration methods (i.e. *Africa fixed hotspot, Africa moving hotspot, Global moving hotspot, and Global palaeomagnetic*) yield mean deviations of 7, 8, 8 and 6° respectively. The average δV_s varies between −1.0 and −1.1 per cent for the different methods. All methods produce similar patterns of LIP eruption sites that cluster around the FSBs at the CMB. Because all methods yield broadly similar results, it is difficult, using presently available data, to select one as 'better than' or 'more appropriate to apply' than the others. The palaeomagnetic frame has one advantage over the others, which is that it can be applied to LIPs as old as the Siberian Traps (251 Myr). Pending the acquisition of more data we recommend that for the Pacific Ocean sites the Pacific mantle frame (Fig. 7) should be used because it corresponds better with both the global palaeomagnetic frame and the observed palaeomagnetic latitude for the Ontong Java LIP. The Pacific mantle frame also avoids the plate closure problems when attempting to relate Pacific LIPs to Africa (Figs 4–6).

5.1 Differences between the LLVPs in (a) marginal gradients and (b) numbers of preserved LIPs

FSBs at the edges of both the African and the Pacific LLVPs are marked by steep gradients close to the 1 per cent slow contour. About

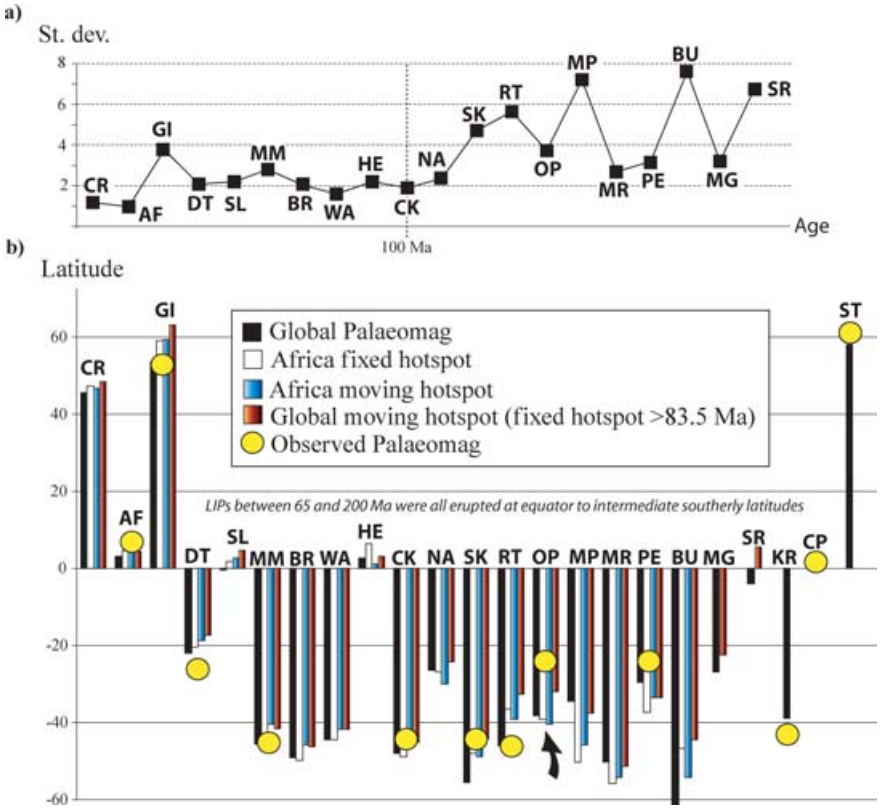

Figure 8. (a) Latitude standard deviation (1σ) between the different reference frames (sorted by age from 15 to 147 Ma) in (b): Comparison of palaeolatitudes from all LIPs (sorted by age) using the *Global palaeomagnetic, Africa fixed hotspot, Africa moving hotspot, Global moving hotspot mantle* and *observed palaeomagnetic* latitudes. A notably large offset between Global palaeomagnetic and observed palaeomagnetic is seen for the 121 Ma Ontong Java (14°) LIP. The Ontong Java offset is reduced to 8° if we compare observed palaeomagnetic with our *Global moving hotspot mantle* frame. Observed palaeomagnetic latitudes are recalculated to a sampling position that coincides with our chosen *in situ* centre for the LIPs (Table 1).

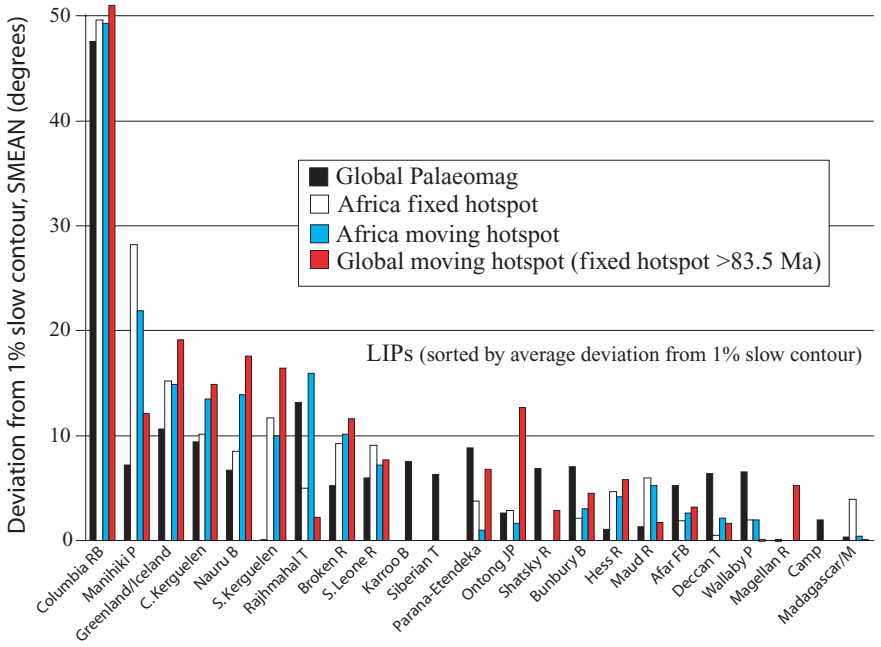

Figure 9. Great circle angles between original LIP eruption sites and the 1 per cent slow contour in the SMEAN shear wave velocity model for 2800 km depth. Angles for the four alternative reconstruction methods are shown (see Figs 4 to 7 and Table 1). All reconstruction methods rotate most LIPs to within 10 degrees of arc of the −1 per cent contour, that for the most part coincides with the highest lateral gradients in shear wave velocity near the CMB. Note that the distance for the Siberian Traps is measured from a small local 1 per cent slow area.

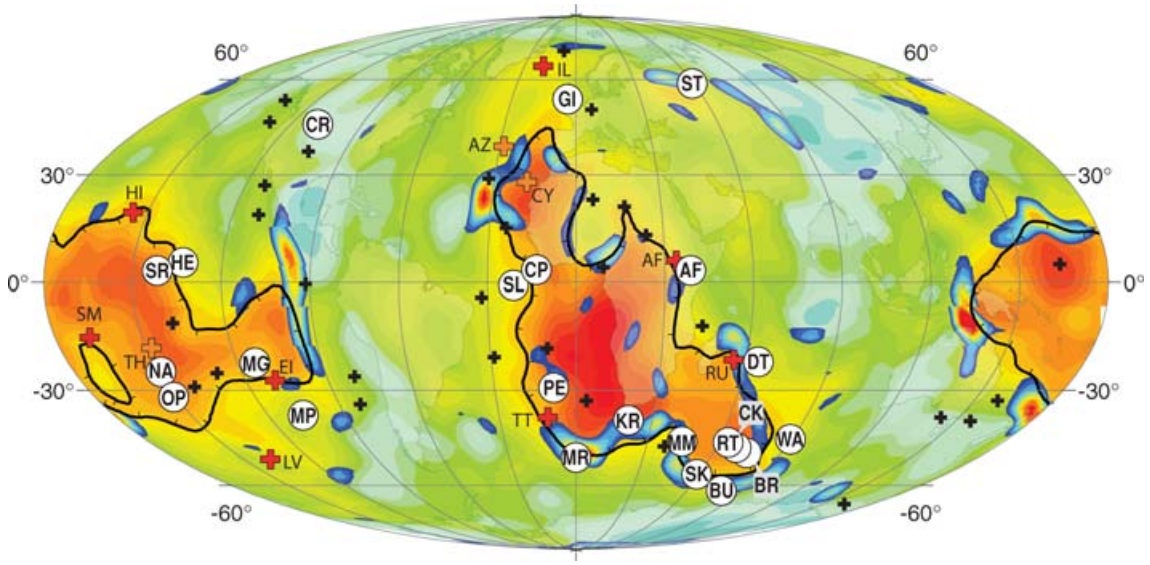

Figure 10. Original LIP eruption sites [palaeomagnetic and global moving/fixed hotspot (for the Pacific) frame, Figs 6 and 7] and hotspots (crosses) on the SMEAN shear wave velocity anomaly model for 2800 km. Hotspots argued to have originated from deep plumes are in red (based on *S*-wave tomography and additional criteria, Courtillot *et al.* 2003; Ritsema & Allen 2003) and light-brown (based on *P*-wave tomography. Easter Islands, Hawaii and Samoa also recognized as deep plumes from *P*-wave tomography; Montelli *et al.* 2004) crosses. There is a strong tendency for LIP and hotspot eruption sites to overlie the high horizontal gradients in seismic velocity peripheral to the 'Africa' and 'Pacific' low-velocity regions (red). The highest horizontal gradients generally lie along the −1 per cent slow contour.

50 per cent of the length of that contour around the African slow region is coincident with very steep velocity gradients as high as 1.6 per cent/degree. Along much of the rest of the length of the contour the gradient is steep but not as steep as in the parts shown in bright colours on Fig. 10. Fifteen projected LIP eruption sites lie close to the FSB of the African LLVP at the CMB. Ten project onto or inside the 1 per cent slow contour. The remaining five are close to but outside the 1 per cent contour. Seven in the southeast form a Kerguelen cluster. On the northeastern margin of the African LLVP there is only one young LIP (AF: Afar at 31 Ma). This may be because older LIPs along this margin may have been subducted during Tethyan ocean evolution.

In the Pacific LLVP less than 50 per cent of the 1 per cent slow contour's length is occupied by very steep gradients (>0.16 per cent/degree). All of the six projected LIP eruption sites of the Pacific region lie close to the 1 per cent slow velocity contour but only two are close to very steep gradient segments of the FSB. The other four are in a region where the slope is steep but does not reach 0.16 per cent/degree, the cut-off value used in our figures.

The western two-thirds of the area in the Pacific that projects vertically downwards to the Pacific LLVP is without restored LIP sites. One of the most westerly restored sites is the Shatsky Rise LIP (SR) in the northwestern Pacific Ocean. The absence of restored LIP sites farther to the west over the Pacific LLVP probably results from subduction of LIPs that once lay on ocean floor to the west of the Shatsky Rise. The importance of subduction in limiting and partly destroying the Pacific record cannot be overemphasized. It has, for example, long been recognized that the Hess Rise Twin was subducted under the Cordillera of North America triggering the Laramide orogeny at *ca.* 80 Ma (Livacarri *et al.* 1981). Similarly the Hikurangi plateau, a twin of the Manihiki plateau has been caught up in an accretionary complex in New Zealand (D. Müller personal communication, 2005).

5.2 Hotspots and the Deep mantle

Analysis so far has been confined to consideration of the positions of LIPs with respect to the CMB at the time of their eruption. Here we extend our analysis to hotspots. Hotspots can be simply, although somewhat imperfectly, defined as 'volcanic provinces other than those of plate boundary zones and those formed by pressure relief melting in intracontinental rifts'. Many hotspots, for example Hawaii (Wilson 1963; Morgan 1971), have long been suggested to overlie plumes that originated at the CMB and some hotspots, for example Tristan and Kerguelen, lie at the ends of plume trails that are linked to LIPs. Analysis here of how hotspots relate to the structure of the deep mantle does not use the most comprehensive catalogue of *ca.* 140 hotspots (Sengor 1995) because that catalogue, particularly in its African plate section, contains a number of hotspots of shallow origin (Burke 1996). It also needs to be purged of some intracontinental volcanic provinces now known to be better attributed to pressure relief melting in rifts than to be considered hotspots. Instead we used Steinberger's (2000) catalogue of 44 hotspots.

Thorne *et al.* (2004) showed that some of those hotspots when projected downward reach regions with steep shear wave velocity gradients on the FSB of the Pacific LLVP. We address the relationship of the 44 hotspots to the FSBs at the CMB in a somewhat different way by calculating the angular distances between the projected hotspots and the 1 per cent slow contour (Table 2, Figs 10 and 11). Courtillot *et al.* (2003) and Ritsema and Allen (2003) concluded respectively on the basis of underlying low shear wave velocities in both the upper and lower mantle and by using a variety of other criteria that only seven and eight hotspots (IL, LV, SM, TT, AF, RU, HI and EI) had a deep plume origin (Fig. 10). Montelli *et al.* (2004) using *P*-wave tomography added a few more hotspots (TH, AZ and CY) to those of deep origin. Here we show that most hotspots of arguably deep origin in Fig. 10 overlie the margins of one or other of the two LLVPs close to the CMB. Eight (EI, HI, RU, AF, TT, SM,

Table 2. Hotspots (Steinberger 2000) sorted by the angular distance from the 1 per cent slow contour. Column headings are as in Table 1. Hotspot entries in bold have been argued to a have a deep plume origin and they are all underlain by slow velocities at the CMB.

Name	Symbol	Age	Lat	Long	δV_S	Angle
Yellowstone	YS	15	44.6	−110.5	1.0	42
Raton	RT	20	37	−104	0.9	38
Bowie	BO	28	53	−135	0.8	35
Balleny (Buckle Island)	BI	36	−66.8	163.3	0.9	34
Cobb (Axial Smt.)	CO	43	46	−130	0.7	31
Guadelupe	GL	25	27	−113	0.4	29
Jan Mayen (Beerenberg)	JM	210	71.1	−8.2	0.3	27
Socorro Island	SI	25	18.7	−111	0.5	22
Iceland	**IL**	**60**	**65**	**−19**	**−0.5**	**21**
East Australia	AU	50	−38	143	1.0	19
Tahiti (Mehetia)	**TH**	**5**	**−17.9**	**−148.1**	**−1.9**	**−17**
Tasmanid	TM	50	−39	156	1.0	15
Vema	VM	40	−33	4	−2.6	−15
Juan Fernandez	JF	30	−34	−82	0.4	14
Fernando	FD	70	−4	−32	−0.1	14
Eifel	EL	40	50	7	0.2	14
San Felix	SF	30	−26	−80	0.6	13
Louisville	**LV**	**120**	**−51**	**−138**	**−0.2**	**13**
Caroline	CA	80	5	164	−2.5	−10
Trindade	TD	120	−20.5	−28.8	−0.3	10
Lord Howe	LH	50	−33	159	0.3	8
Kerguelen	KG	117	−49	69	−1.8	−8
Galapagos (Fern.I.)	GA	85	−0.4	−91.5	0.7	7
St Helena	SH	100	−18	−10	−2.1	−7
Azores (Pico)	**AZ**	**100**	**38.5**	**−28.4**	**−0.0**	**7**
Marquesas	MQ	9	−11	−138	−1.7	−7
Comores (Karthala)	CM	63	−11.8	43.3	−0.4	7
Canary	**CY**	**65**	**28**	**−18**	**−1.9**	**−6**
Macdonald (Smt.)	MD	120	−29	−140.2	−1.5	−6
Marion Island	MI	195	−46.9	37.8	−0.5	5
New England	NE	120	29	−32	−0.2	4
Hoggar	HG	20	23	6	−0.3	3
Pitcairn	PC	8	−25	−129	−1.4	−3
Meteor	MT	120	−52	1	−0.1	3
Samoa	**SM**	**14**	**−15**	**−168**	**−1.1**	**−2**
Tristan	**TT**	**125**	**−38**	**−11**	**−1.2**	**−2**
East Africa	**AF**	**40**	**6**	**34**	**−0.7**	**2**
Cameroon	CR	31	4.2	9.2	−1.5	−2
Reunion	**RU**	**67**	**−21.2**	**55.7**	**−1.3**	**−1**
Tibesti	TB	80	21	17	−0.8	1
Hawaii (Kilauea)	**HI**	**100**	**19.4**	**−155.3**	**−1.0**	**−1**
Darfur	DF	140	13	24	−1.0	1
Cape Verde	CV	20	15	−24	−1.2	0
Easter Islands	**EI**	**68**	**−27.1**	**−109.3**	**−0.9**	**0**

CY and AZ) plot on or very near to the projected 1 per cent slow contour (<7°) and six of those hotspots lie close to very steep shear wave velocity gradients on that contour.

6 SYNTHESIS AND DISCUSSION

We have found that most LIPS project radially to sites within ±10° of one or other of the FSBs of the LLVP margins at the CMB (Fig. 9). We have thus shown that plume sources of the past 200 Myr have been concentrated in belts straddling the peripheries of the two LLVPs at the CMB. The spatial correlation between the surface features and the edge of the African LLVP at the CMB is particularly clear. LIPs related to the African LLVP (except the Early Tertiary North Atlantic LIP [GI in Fig. 10]), ranging in age from 31 Ma (Afar) to 200 Ma (CAMP) as well as the majority of hotspots project radially downwards onto or close to the FSB at the CMB. In Fig. 12 we also show a NNE trending shear wave tomographic profile that intersects the restored positions at the CMB of the Maud Rise, Afar and Siberian Trap plume sources. The profile cuts across the African LLVP showing it as extending to approximately 1500 km above the CMB. The African LLVP is marked not only by the strong marginal horizontal gradient characteristic of the FSBs at the CMB but also by sharp-edged vertical relief of hundreds of kilometres (Ni *et al.* 2002). Fig. 10 shows that no LIPs or hotspots project radially downwards onto the highest parts of the African LLVP. Projections are concentrated only along its margins where that margin lies at the CMB.

How the deep mantle plumes that generated LIPs and hotspots have been sourced from within the marginal belts of one or other LLVP for at least 200 Myr (the age of the CAMP LIP) remains unexplained. What are possible dynamic reasons for the concentration of plume sources within the two belts? We first consider current understanding of the structure of the D″ zone, with an emphasis on aspects related to our question.

6.1 Structure of the D″ zone

The D″ zone is characterized by a combination of thermal and compositional variations, with complexity added by the presence of a phase change. A thermal boundary layer at the base of the mantle in the D″ zone is required by all models. The energy needs of the geodynamo in the Earth's core, although somewhat uncertain, call for heat to be conducted across the CMB from the core to the mantle. Temperature estimates for the core side of the CMB are about 4000 K (Boehler 1996) and thus substantially higher than estimates of temperature in the mantle just above the D″ for which a value of about 2500 K has been obtained by extrapolation from below the lithosphere along an adiabat with appropriate thermal expansivity profile (see e.g. Schubert *et al.* 2001, for a recent review). The difference indicates a temperature drop of >1000 K across the CMB.

Evidence is accumulating for both a phase change and compositional variation in the D″ zone. The presence of a phase change is suggested by the recent experimental production of a post-perovskite phase transition in $MgSiO_3$ (Murakami *et al.* 2004). That phase change is likely to occur 200–300 kilometres above the CMB. Such a phase change can explain the occurrence of a seismic discontinuity about 200 km above the CMB (Sidorin *et al.* 1999a). Both calculations (Tsuchiya *et al.* 2004) and preliminary experiments (Hirose & Fujita 2005) indicate a large positive Clapeyron slope (7.5 MPa K^{-1} or more) for the phase change. Similar values for depth and Clapeyron slope were obtained by Sidorin *et al.* (1999b) by comparing the results of convection modelling with seismic observations. They found that best fits to the observed waveforms were obtained for phase transitions characterized by a Clapeyron slope of about 6 MPa K^{-1} and an elevation above the CMB of ∼150 km. A large positive Clapeyron slope, in combination with substantial temperature variations implicit in a laterally variable thermal boundary layer is suggestive of major depth variation for the phase boundary. That variation could also explain why the D″ seismic discontinuity is primarily observed in the regions of positive shear wave velocity anomaly that have been suggested to contain subducted material which is likely colder than average material at D″ depths. In hotter regions the pressure required to reach the phase transition might be greater than that at the CMB and the post-perovskite layer could be absent. In colder regions, the post-perovskite transition is expected

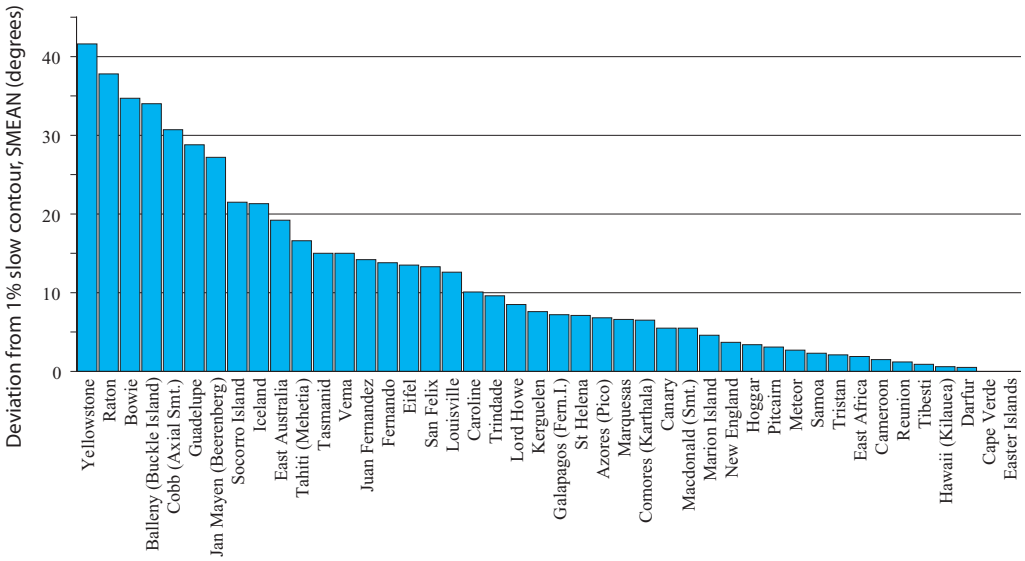

Figure 11. Great circle angles between hotspots and the 1 per cent slow contour in the SMEAN shear wave velocity model for 2800 km depth (see Fig. 2 and Table 2).

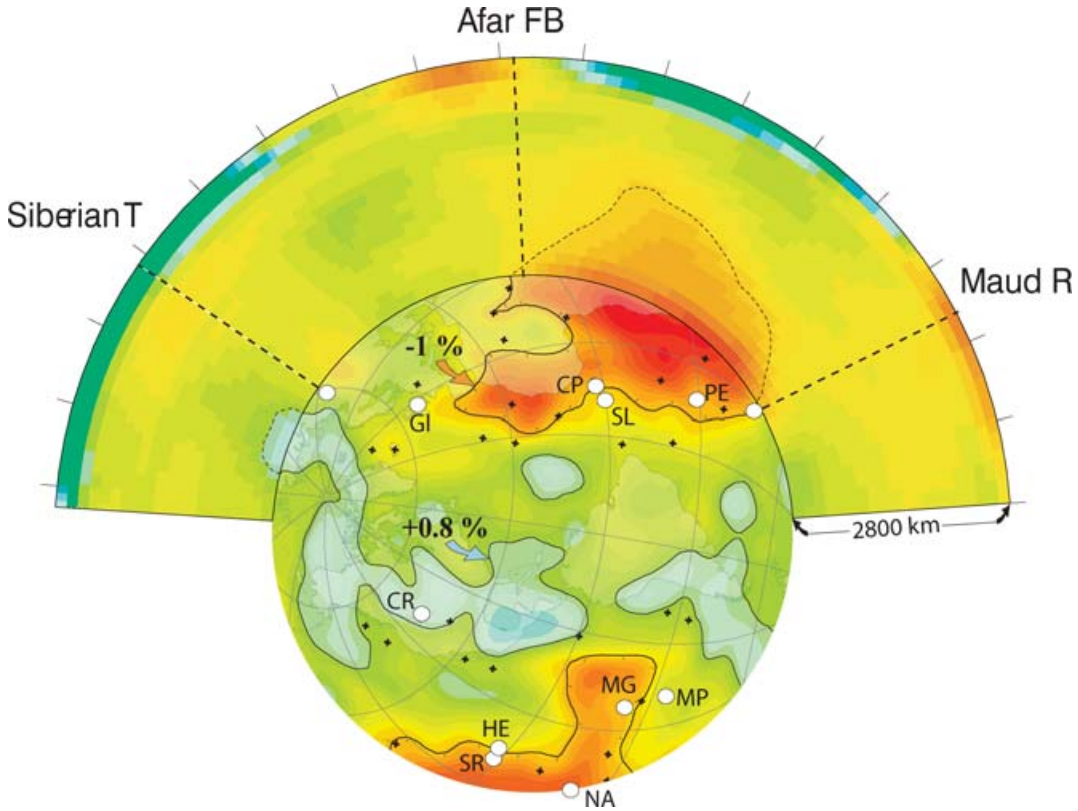

Figure 12. Some restored LIP eruption sites (from Fig. 10), hotspots (crosses) and continental outlines projected onto the CMB (SMEAN model). We also show the 1 per cent slow and the 0.8 per cent fast contours at the CMB and a 'vertical' tomographic profile based on SMEAN (0–2800 km vertical scale). δV_s scale as all other diagrams.

to occur twice in that case, with a narrow layer of perovskite underlying the post-perovskite layer, because the CMB is presumed to be isothermal.

A number of studies involving seismological considerations favour interpretation of variations within the D″ zone as related to chemical composition:

(1) Both Ni *et al.* (2002) and Wang & Wen (2004) found that the African LLVP has sharp and steeply dipping edges that are best explained as compositionally controlled.

(2) Mao *et al.* (2006) show that ultralow-velocity patches observed by seismology may be due to iron enrichment in post-perovskite.

(3) Masters *et al.* (2000) found that *S*-wave and bulk sound anomalies were anticorrelated in the lowermost mantle. Those anomalies should be perfectly correlated if solely of thermal origin.

(4) Explicit density models based on seismology including normal modes (Ishii & Tromp 2004) indicate positive density anomalies in the two LLVPs of the D″ zone. Those anomalies are best attributed to compositionally denser material.

(5) While such explicit density models remain controversial (Kuo & Romanowicz 2002), a recent dynamic model by Steinberger & Holme (2006) features a very similar D″ density structure, both in pattern and in amplitude. They found that, without such a layer of denser material, both CMB relief (Garcia & Souriau 2000) and excess ellipticity (Mathews *et al.* 2002) tend to be predicted too high. Computations better fit observations if relief that would be otherwise at the CMB in the models is compensated due to density variations in the lowermost mantle.

(6) Tan & Gurnis (2005) show that piles of chemically distinct material on the CMB with steep edges and consistent with the seismological observations, as well as geodynamical, mineralogical and geochemical constraints can persist for long periods of geological time.

(7) McNamara & Zhong (2005) show that Earth's subduction history can lead to thermochemical structures similar in shape to the observed large lower-mantle velocity anomalies.

In addition to seismological considerations it can be argued that if plumes arise from the lowermost mantle, their rather low excess temperature compared with the implied temperature drop across D″ indicates that D″ is not just a thermal boundary: Both Albers & Christensen (1996) and Farnetani (1997) favoured the explanation that plumes rise from the top of a chemically distinct layer at the base of the mantle, since it is far easier to account for the relatively modest temperature excess of hotspot melts by having a much weaker thermal boundary layer as plume source.

6.2 Speculations on possible causes and implications of the concentration of plume sources close to the CMB at the margins of the LLVPs

Here we speculate about why the sources of plumes that have generated LIPS over the past 200 Myr fall into two narrow belts close to the CMB that straddle places where the fast and slow parts of the D″ zone are in contact with each other and with the core. Because of the concentration of the plume sources where core, fast D″ and slow D″ are in contact all three are likely to be involved in some way in plume generation. The role of the core is likely to be dominantly, if not completely, in contributing heat. The roles of the fast and slow parts of the D″ to generating plumes are likely to be in contributing two different kinds of material to the plume.

Juxtaposition of LLVPs, the faster parts of the D″ zone and the core in plume source regions is consistent with isotopic evidence of LIP derivation from a variety of reservoirs. A plume that forms where the three meet might be expected to contain: (i) depleted material from slab graveyards in the faster parts of the D″ zone, (ii) fertile material and noble gases (such as He with a high $^3He/^4He$ ratio) from LLVPs which appear to have been isolated from the rest of the mantle for at least 200 Myr and possibly for very much longer and (iii) some core involvement (Walker & Walker 2005).

There is already some evidence on the basis of a variety of observations, physical and numerical experiments that the CMB below the faster parts of the D″ zone is unlikely to be the source of plumes of deep-seated origin. Those faster regions have been suggested to contain subducted material in 'slab graveyards':

(i) Those regions are likely cold and refractory, thus formation of plumes might be suppressed.

(ii) Slabs might also impede buoyant transit of plumes.

(iii) Formation of plumes might also be suppressed due to large-scale flow of the mantle imposed by plate motions, thinning the thermal boundary layer at the base of the mantle below those regions where plates converge, corresponding to subduction zones on Earth (Gonnermann *et al.* 2004). Their physical experiments were performed in a compositionally homogenous fluid and could be modified in the presence of a chemically distinct basal layer.

Rather, plumes are expected to form at the edge of slab graveyards at the FSB:

(i) Tan *et al.* (2002) found in a numerical experiment that a plume developed in front of a slab moving into the lower mantle.

(ii) In a related experiment Tan *et al.* (2002) found that a plume generated at the CMB under a slab that was moving horizontally just above the CMB was forced to migrate to the edge of the slab.

(iii) Edge-driven convection may occur at steep vertical boundaries. King & Anderson (1998) show that edge-driven down-welling may occur at the steep edges of continental roots, which are colder than the ambient mantle. We speculate here that a similar mechanism may occur at the base of the mantle, causing upwelling at steep edges of LLVPs which are hotter than the ambient mantle.

All these results are consistent with our finding that plumes have erupted only from the FSBs at the edges of the LLVPs and not from the interior of the faster parts of the D″ zone. The Columbia River basalt province, if indeed it is of deep mantle origin, provides an exception.

The slower parts of the D″ zone represented by the two LLVPs have been considered more likely than the fast part to generate mantle plumes (see e.g. Lay 2005, fig. 1) but we have found *no* LIPs and few hotspots that project down onto the interior, more elevated, surfaces of the LLVPs (Figs 10 and 12). Numerical results indicate that the post-perovskite phase change enhances the occurrence of thermal instabilities (Nakagawa & Tackley 2004). If this phase change is absent or occurs closer to the CMB in the central parts of the LLVPs, it could be that thermal instabilities and plumes are more likely to occur at the edges rather than the centres. However, Yamagishi *et al.* (2006) found that in 3-D spherical geometry that phase transition has little influence on the dynamics of convection.

The LLVPs are sometimes called upwellings but this may be misleading. Our analysis suggests that within resolution the areas of the LLVPs at the CMB have remained constant during the past 200 Myr which is consistent with the idea that the volumes have also remained constant. Substantial volume change of an LLVP requires addition or subtraction of material. The absence of LIPs and hotspots at the surface above the LLVPs shows that there is no evidence that material has left those structures and the foundering of subducted slabs, the only known way of adding material to the lower mantle, has been discerned only over the faster parts of the D″ zone. Because the thermochemical structure and volume of the LLVPs do not appear to have changed over the past 200 Myr any effects of a phase change are also unlikely to have changed within those provinces over a similar interval.

Episodicity and sporadicity of plume origin calls for the generation of new instabilities at the CMB. Numerous reasons have been suggested for that process and many more can be readily imagined:

(i) Plumeheads that generated the LIPs of the past 200 Myr appear to have risen relatively quickly. As a result of non-linear rheology, large stresses may have reduced the effective viscosity around plumeheads (Weinberg & Podladchikov 1994; Larsen & Yuen 1997; van Keken 1997), thus increasing rise speed. Relatively large amounts of heat could have been released within a short time. It would then take some time until the next instability could form.

(ii) Tomographic models indicate that slabs do not continually penetrate the lower mantle (Fukao *et al.* 2001). Temporal variations in the passage of slabs into the lower mantle and, in the extreme case mantle avalanches (Tackley *et al.* 1993) may contribute to episodicity and sporadicity in the generation of new plumes.

7 CONCLUSIONS

(1) Eruption sites for approximately 90 per cent of all LIPs of the past 200 Myr project radially downwards onto the CMB at places where it is intersected by the FSBs at the margins of one or other of the two LLVPs which form the deep mantle's most prominent features.

(2) We infer that nearly all LIPs and some hotspots have been generated by plumes rising from the CMB at an FSB within the D″ zone.

(3) Four reference frames used to restore LIPs to their eruption sites all bring the projected LIP sites close to the FSBs. Present data and methods do not permit discrimination among those reference frames.

(4) D″ zone FSBs lie on both the 1 per cent slow contour of shear wave velocity and the maximum horizontal gradient in shear wave velocity.

(5) The spatial link between LIPs of different ages and the FSBs at the CMB indicates that deep mantle large-scale structure is long-lived and has not changed (within our resolution) as far back as at least the time of the eruption of the Siberian Traps (251 Ma).

(6) The ages and short eruption times of LIPs (*ca.* 1 My) indicate that plume sources have developed and decayed on a timescale much shorter than 200 My.

(7) The longevity of D″ heterogeneities provides additional evidence that they cannot be purely thermal in origin but have a compositional component.

(8) LIPs in the 200 to 65 Myr range were erupted at equatorial or intermediate southerly latitudes. This is consistent with control by deep mantle structure.

ACKNOWLEDGMENTS

We thank the Norwegian Research Council, Statoil and NGU for financial help (PETROMAKS Frontier Science and Exploration no. 163395/S30 - www.geodynamics.no). We also thank C. Mac Niocaill and an anonymous referee for comments, and H. Schmeling for helpful suggestions.

REFERENCES

Albers, M. & Christensen, U.R., 1996. The excess temperature of plumes rising from the core-mantle boundary, *Geophys. Res. Lett.,* **23,** 3567–3570.

Becker, T.W. & Boschi, L., 2002. A comparison of tomographic and geodynamic mantle models, *Geochem. Geophys. Geosys.,* **3,** 2001GC000168.

Bergen, J.A., 2004. Calcareous nannofossils from ODP Leg 192, Ontong Java Plateau, in *Origin and Evolution of the Ontong Java Plateau,* Vol. 229, pp. 113–132, eds Fitton, J. G., Mahoney, J.J., Wallace, P.J. & Saunders, A.D., Geol. Soc. Spec. Publ.

Boehler, R., 1996. Melting temperature of the Earth's mantle and core: Earth's thermal structure, *Ann. Rev. Earth Planet. Sci.,* **24,** 15–40.

Burke, K., 1996. The African Plate, *S. African J. Geology,* **99,** 341–409.

Burke, K. & Torsvik, T.H., 2004. Derivation of large igneous provinces of the past 200 million years from long-term heterogeneities in the deep mantle, *Earth planet. Sci. Lett.,* **227,** 531–538.

Burke, K., MacGregor-Duncan, D.S. & Cameron, N.R., 2003. Africa's petroleum systems: four tectonic 'aces' in the past 600 million years, in *Petroleum geology of Africa; new themes and developing technologies,* Vol. 207, pp. 21–60, eds Arthur, T., MacGregor, D.S. & Cameron, N.R., Geol. Society Lond. Special Publ.

Chambers, L.M., Pringle, M.S. & Fitton, J.G., 2004. Phreatomagmatic eruptions on the Ontong Java Plateau: an Aptian $^{40}Ar/^{39}Ar$ age for volcaniclastic rocks at ODP Site 1184, in *Origin and Evolution of the Ontong Java Plateau,* Vol. 229, pp. 325–331. eds Fitton, J.G., Mahoney, J.J., Wallace, P.J. & Saunders, A.D. Geol. Soc. Spec. Publ.

Courtillot, V., Davaille, A., Besse, J. & Stock, J., 2003. Three distinct types of hotspots in the Earth's mantle, *Earth planet. Sci. Lett.,* **205,** 295–308.

Davaille, A., Stutzmann, E., Silveira, G., Besse, J. & Courtillot, V., 2005. Convective patterns under the Indo-Atlantic, *Earth planet. Sci. Lett.,* **239,** 233–252.

Duncan, R.A. & Clague, D.A., 1985. Pacific Plate motion recorded by linear volcanic chains, in *The Pacific Ocean,* pp. 89–121, eds Nairn, A.E.M., Stehli, F.G. & Uyeda, S. Plenum Press, New York.

Eldholm, O. & Coffin, M.F., 2000. Large igneous provinces and plate tectonics, in *The History and Dynamics of Global Plate Motions,* pp. 309–326, eds Richards, M.A., Gordon, R.G. & van der Hilst, R.D. American Geophysical Union, Washington.

Farnetani, C.G., 1997. Excess temperature of mantle plumes: The role of chemical stratification across D″, *Geophys. Res. Lett.,* **24,** 1583–1586.

Foulger, G.R., Natland, J.H., Presnall, D.C. & Anderson, D.L., 2005 (Editors), *Plates, Plumes & Paradigms,* Geological Society of America Special Volume 388.

Fukao, Y., Widiyantoro, S. & Obayashi, M., 2001. Stagnant slabs in the upper and lower mantle transition region, *Rev. Geophys.,* **39,** 291–323.

Garcia, R. & Souriau, A., 2000. Amplitude of the core-mantle boundary topography estimated by stochastic analysis of core phases, *Phys. Earth planet. Inter.,* **117,** 345–359.

Garnero, E.J., Revenaugh, J., Williams, Q., Lay, T. & Kellogg, L.H., 1998. Ultralow velocity zone at the cor-mantle boundary, in *The Core-Mantle Boundary Region,* Vol. 28, pp. 319–334, eds Gurnis, M., Wysession, M.E., Knittle, E. & Buffet, B.A., AGU, Washington, DC, Geodyn. Ser.

Gonnermann, H.M., Jellinek, A.M., Richards, M.A. & Manga, M., 2004. Modulation of mantle plumes and heat flow at the core-mantle boundary by plate-scale flow: Results from laboratory experiments, *Earth planet. Sci. Lett.,* **226,** 53–67.

Grand, S.P., 2002. Mantel shear-wave tomography and the fate of subducted slabs, *Phil. Trans. R. Soc. Lond., Ser. A,* **360,** 2475–2491.

Hirose, K. & Fujita, Y., 2005. Clapeyron slope of the post-perovskite phase transition in $CaIrO_3$, *Geophys. Res. Lett.,* **32,** L13313, doi:10.1029/2005GL023219.

Ishii, M. & Tromp, J., 2004. Constraining large-scale mantle heterogeneity using mantle and inner-core sensitive normal modes, *Phys. Earth planet. Int.,* **146,** 113–124.

Jokat, W., Boebel, T., König, M. & Meyer, U., 2003. Timing and geometry of early Gondwana breakup, *J. geophys. Res.,* **108**(B9), 2428, doi:10.1029/2002JB001802.

King, S.D. & Anderson, D.L., 1998. Edge-driven convection, *Earth planet. Sci. Lett.,* **160,** 289–296.

Kuo, C. & Romanowicz, B., 2002. On the resolution of density anomalies in the Earth's mantle using spectral fitting of normal-mode data, *Geophys. J. Int.,* **150,** 162–179.

Larsen, T.B. & Yuen, D.A., 1997. Fast plumeheads: Temperature-dependent versus non-Newtonian rheology, *Geophys. Res. Lett.,* **24,** 1995–1998.

Lay, T., 2005. The deep mantle thermo-chemical boundary layer: the putative mantle plume source, in *Plates, Plumes & Paradigms,* Vol. 388,

pp. 193–205, eds Foulger, G.R., Natland, J.N., Presnall, D.C. & Anderson, D.L., Geological Society of America Special.

Livacarri, R., Burke, K. & Sengor, A.M.C., 1981. Was the Laramide orogeny related to the subduction of an oceanic plateau?, *Nature,* **289,** 276–278.

Mao, W.L. *et al.,* 2006. Iron-rich post-perovskite and the origin of ultralow-velocity zones, *Science,* **312,** 564–565.

Marzoli, A., Renne, P.R., Piccirilo, E.M., Ernesto, M., Bellieni, G. & De Min, A., 1999. Extensive 200-million-year-old continental flood basalts of the Central Atlantic Magmatic Province, *Science,* **284,** 616–618.

Masters, G., Laske, G., Bolton, H. & Dziewonski, A., 2000. The relative behavior of shear velocity, bulk sound speed, and compressional velocity in the mantle: implications for chemical and thermal structure, in *Seismology and Mineral Physics,* Vol. 117, pp. 63–87, eds Karato, S., Forte, A.M., Liebermann, R.C., Masters, G. & Stixrude, L., AGU Geophys. Monogr. Ser.

Mathews, P.M., Herring, T.A. & Buffett, B.A., 2002. Modeling of nutation and precession: new nutation series for nonrigid Earth and insights into the Earth's interior, *J. geophys. Res.,* **107,** doi:10.1029/2001JB000390.

McNamara, A.K. & Zhong, S., 2005. Thermochemical structures beneath Africa and the Pacific Ocean, *Nature,* **437,** 1136–1139, doi:10.1038/nature04066.

Montelli, R., Nolet, G., Dahlen, F., Masters, G., Engdahl, E. & Hung, S., 2004. Finite-frequency tomography reveals a variety of mantle plumes, *Science,* **303,** 338–343.

Morgan, W., 1971. Convection plumes in the lower mantle, *Nature,* **230,** 42–43.

Müller, R.D., Royer, J.-Y. & Lawver, L.A., 1993. Revised plate motions relative to the hotspots from combined Atlantic and Indian Ocean hotspot tracks, *Geology,* **16,** 275–278.

Murakami, M., Hirose, K., Kawamura, K., Sata, N. & Ohishi, Y., 2004. Post-perovskite phase transition in $MgSiO_3$, *Science,* **304,** 855–858.

Nakagawa, T. & Tackley, P.J., 2004. Effects of a perovskite-post perovskite phase change near core-mantle boundary in compressible mantle convection, *Geophys. Res. Lett.,* **31,** L16611, doi:10.1029/2004GL020648.

Ni, S., Tan, E., Gurnis, M. & Helmberger, D., 2002. Sharp sides to the African superplume, *Science,* **296,** 1850–1852.

Norton, I.O., 2000. Global hotspot reference frames and plate motion, in *The History and Dynamics of Global Plate Motions,* pp. 309–326, eds Richards, M.A., Gordon, R.G. & van der Hilst, R.D. American Geophysical Union, Washington, DC.

O'Neill, C., Müller, R.D. & Steinberger, B., 2005. On the uncertainties in hotspot reconstructions, and the significance of moving hotspot reference frames, *Geochem. Geophys. Geosyst.,* **6,** Q04003, doi:10.1029/2004GC000784.

Parkinson, I.J., Schaefer, B.F. & Arculus, R.J., 2002. A lower mantle origin for the world's biggest LIP? A high precision Os isotope isochron from Ontong Java Plateau basalts drilled on ODP Leg 192, *Geochim. Cosmochim. Acta,* **66** (Suppl.), 580.

Ritsema, H.J., van Heijst, J.H. & Woodhouse, J.H., 1999. Complex shear velocity structure beneath Africa and Iceland, *Science,* **286,** 1925–1928.

Ritsema, J. & Allen, R.M., 2003. Frontier: The elusive mantle plume, *Earth planet. Sci. Lett.,* **207,** 1–12.

Richards, M.A. & Engebretson, D.C., 1992. Large scale mantle convection and the history of subduction, *Nature,* **355,** 437–440.

Schubert, G., Turcotte, D.L. & Olson, P., 2001. *Mantle Convection in the Earth and Planets,* Cambridge University Press, Cambridge.

Sengor, A.M.C., 1995. Sedimentation and tectonics of fossil rifts, in *Tectonics of Sedimentary Basins,* pp. 53–118, eds Raymond, F. & Busby, C.T., Blackwell Sciences, Oxford, England.

Sengor, A.M.C. & Natalin, B.A., 2001. Rifts of the World, *Geol. Soc. America Spec. Paper,* **352** 389–482.

Sidorin, I., Gurnis, M. & Helmberger, D.V., 1999a. Evidence for a ubiquitous seismic discontinuity at the base of the mantle, *Science,* **286,** 1326–1331.

Sidorin, I., Gurnis, M. & Helmberger, D.V., 1999b. Dynamics of a phase change at the base of the mantle consistent with seismological observations, *J. geophys. Res.,* **104,** 15 005–15 023.

Sleep, N.H., 1997. Lateral flow and ponding of starting plume material. *J. geophys. Res.,* **102,** 10 001–10 012.

Steinberger, B., 2000. Plumes in a convecting mantle: Models and observations for individual hotspots, *J. geophys. Res.,* **105,** 11 127–11 152.

Steinberger, B. & Holme, R., 2006. Mantle flow models with core-mantle boundary constraints: Evidence for chemical heterogeneities in the lowermost mantle, *J. geophys. Res.,* submitted.

Steinberger, B., Sutherland, R. & O'Connell, R.J., 2004. Prediction of Emperor-Hawaii seamount locations from a revised model of plate motion and mantle flow, *Nature,* **430,** 167–173.

Tackley, P.J., Stevenson, D.J., Glatzmaier, G.A. & Schubert, G., 1993. Effects of an endothermic phase transition at 670 km depth in a spherical model of convection in the Earth's mantle, *Nature,* **361,** 699–704.

Tan, E., Gurnis, M. & Han, L., 2002. Slabs in the lower mantle and their modulation of plume formation, *Geochem. Geophys. Geosyst.,* **3**(11), 1067, doi:10.1029/2001GC000238.

Tan, E. & Gurnis, M., 2005. Metastable superplumes and mantle compressibility, *Geophys. Res. Lett.,* **32,** L20307, doi:10.1029/2005GL024190.

Thorne, M.S., Garnero, E.J. & Grand, S., 2004. Geographic correlation between hot spots and deep mantle lateral shear-wave velocity gradients, *Phys. Earth planet. Inter.,* **146,** 47–63.

Torsvik, T.H., Müller, R.D., Van der Voo, R., Steinberger, B. & Gaina, C., 2006. Global plate motion frames: toward a unified model, *Earth Science Reviews* (in review) - submitted version available at: http://www.geodynamics.no/guest/GlobalFrames_ESR.pdf

Tsuchiya, T., Tsuchiya, J., Umemoto, K. & Wentzcovitch, R.M., 2004. Phase transition in $MgSiO_3$. perovskite in the earth's lower mantle, *Earth planet. Sci. Lett.,* **224,** 241–248.

van Keken, P., 1997. Evolution of starting mantle plumes: a comparison between numerical and laboratory models, *Earth planet. Sci. Lett.,* **148,** 1–11.

Van der Voo, R., Spakman, W. & Bijwaard, H., 1999. Mesozoic subducted slabs under Siberia, *Nature,* **397,** 246–249.

Walker, R.J. & Walker, D.L., 2005. Does the Core Leak?, *EOS, Trans. Am. geophys. Un.,* **86,** 237–242.

Wang, Y. & Wen, L., 2004. Mapping the geometry distribution of a very low velocity province at the base of the Earth's mantle, *J. geophys. Res.,* **109,** B10305, doi:10.1029/2003/JB002674.

Weinberg, R.F. & Podladchikov, Y., 1994. Diapiric ascent of magmas through power law crust and mantle, *J. geophys. Res.,* **99,** 9543–9559.

Wilson, J.T., 1963. Evidence from islands on the spreading of ocean floors, *Nature,* **197,** 536–538.

Yamagishi, Y., Yanagisawa, T., Stegman, D. & Yamano, Y., 2006. Thermal state in the mantle modified by the effects of PPV phase transition, *10th Symposium on Study of the Earth's Deep Interior,* July 9–14, Prague, Czech Republic (abstract).